frontiers in Physics

ORIGINAL RESEARCH
published: 23 December 2021
doi: 10.3389/fphy.2021.786357

Bright Soliton and Bright–Dark Soliton Pair in an Er-Doped Fiber Laser Mode-Locked Based on In_2Se_3 Saturable Absorber

Qin Wei [1,2†], Xile Han [3†], Huanian Zhang [1,4], Chonghui Li [5,6], Chao Zhang [1] and Baoyuan Man [1]**

[1]School of Physics and Electronics, Shandong Normal University, Jinan, China, [2]Shandong University of Traditional Chinese Medicine, Jinan China, [3]Institute of Photonics Technology, Jinan University, Guangzhou, China, [4]School of Physics and Optoelectronic Engineering, Shandong University of Technology, Zibo, China, [5]Shandong Key Laboratory of Biophysics, Institute of Biophysics, Dezhou University, Dezhou, China, [6]Institute for Integrative Nanosciences, IFW Dresden, Dresden, Germany

The output power in ultrafast fiber lasers is usually limited due to the lack of a versatile saturable absorber with high damage threshold and large modulation depth. Here we proposed a more efficient strategy to improve the output energy of erbium-doped fiber laser based on indium selenide (In_2Se_3) prepared by using the physical vapor deposition (PVD) method. Finally, stable mode-locked bright pulses and triple-wavelength dark–bright pulse pair generation were obtained successfully by adjusting the polarization state. The average output power and pulse energy were 172.4 mW/101 nJ and 171.3 mW/100 nJ, which are significantly improved compared with the previous work. These data demonstrate that the PVD-In_2Se_3 can be a feasible nonlinear photonic material for high-power fiber lasers, which will pave a fresh avenue for the high-power fiber laser.

Keywords: Indium selenide (In_2Se_3), saturable absorber(SA), physical vapor deposition, mode-locked fiber lasers, soliton

OPEN ACCESS

Edited by:
Yufei Ma,
Harbin Institute of Technology, China

Reviewed by:
Ahmed Al-Masoodi,
American University of Kuwait, Kuwait
Xingliang Li,
Hebei Normal University, China

***Correspondence:**
Chao Zhang
czsdnu@126.com
Baoyuan Man
byman@sdnu.edu.cn

†These authors have contributed equally to this work

Specialty section:
This article was submitted to Optics and Photonics, a section of the journal Frontiers in Physics

Received: *30 September 2021*
Accepted: *24 November 2021*
Published: *23 December 2021*

Citation:
Wei Q, Han X, Zhang H, Li C, Zhang C and Man B (2021) Bright Soliton and Bright–Dark Soliton Pair in an Er-Doped Fiber Laser Mode-Locked Based on In_2Se_3 Saturable Absorber. Front. Phys. 9:786357. doi: 10.3389/fphy.2021.786357

INTRODUCTION

Recently, ultra-fast mode-locked fiber lasers with the virtues of miniaturization, good stability, and beam quality have attracted great attention due to promising applications in industrial manufacturing, biomedicine, defense, optical imaging, and nonlinear optical conversion [1–14]. Especially when studying various nonlinear phenomena, high-power mode-locked fiber lasers often serve as ideal platforms and powerful experimental tools. As the key nonlinear optical element in the passively mode-locked laser, excellent saturable absorbers (SAs) have always been the goal of scientific researchers [15]. At present, various types of two-dimensional (2D) materials were widely employed as passive SAs in mode-locked fiber lasers [16–35]. As a novel two-dimensional layered material, transition metal dichalcogenides (TMDs MoS_2, WS_2, $MoSe_2$, and WSe_2) [19–23] show layer-number-dependent bandgap properties and exhibit a huge potential in nanoelectronics, optical sensor, optoelectronics, and other fields. However, due to the limited carrier mobility of a single layer, its wide application was restricted. Recently, topological insulators (Bi_2Se_3, Bi_2Te_3, and Sb_2Te_3) [24–26] with large modulation depth and excellent optical nonlinearity have aroused great interest in laser photonics. Additionally, black phosphorus with an adjustable direct band gap is widely used in intermediate infrared optoelectronic materials [30–32]. Due to the high nonlinear optical response and the fast recovery time, the ZnO is considered to be an ideal SA [35]. Regretfully, the output power of fiber

lasers based on various broadband SAs was limited to tens of milliwatts due to a low laser damage threshold. Therefore, it is of vital importance to improve the output power of ultrafast fiber lasers.

Most recently, In_2Se_3 with crystalline polymorphism and diverse electronic properties has attracted extensive attention [36–41], which is beneficial to many laser photonic applications. In ultrafast photonic applications, Yan *et al.* fabricated α-In_2Se_3 as SA by magnetron sputtering deposition method and then inserted SA into erbium-doped fiber laser. They finally obtained soliton pulses with maximum average power and single pulse energy of 83.2 mW and 2.03 nJ for erbium-doped fiber laser (EDFL), respectively [42]. Although scientists have conducted extensive research on In_2Se_3, few have been done on nonlinear optical properties to be used as SA for high-power operations.

Generally, 2D In_2Se_3 nanostructures can be prepared by using the mechanical exfoliation (ME) method [29]. However, the size and the thickness of In_2Se_3 nanosheets obtained by the ME method are uncontrollable, and this leads to further limiting the optical response. Additionally, the chemical vapor deposition (CVD) and the physical vapor deposition (PVD) methods were also successfully employed for fabricating In_2Se_3 nanoflakes [43, 44]. Compared with other methods, the PVD method could accurately control the thickness of In_2Se_3 nanoflakes. The PVD-In_2Se_3 exhibits high crystallinity that is beneficial to improve the laser damage threshold. Moreover, the PVD method could achieve highly uniform large-area films, which could further improve the nonlinear optical properties of SA.

In this paper, few-layered In_2Se_3 nanoflakes were successfully fabricated with the PVD method, which showed a high laser damage threshold and excellent nonlinear saturable absorption characteristics. We estimated that the damage threshold of this proposed SA reached up to 50 mJ/cm^2 at the highest pump power in our experiment. The modulation depth of 19% and the saturable intensity of 7.9 MW/ cm^2 are obtained. Stable mode-locked bright pulses and triple-wavelength dark–bright pulses were obtained successfully in our EDFL. The experimental results indicate that In_2Se_3 is a potential SA in the large-energy mode-locked fiber laser application and also demonstrate that the PVD method can be an excellent way for studying high-performance SAs.

FABRICATION AND CHARACTERIZATION OF IN_2SE_3 SA

High-quality In_2Se_3 nanoflakes were prepared by the PVD method, which was similar to our previous reports [45]. The few-layered In_2Se_3 nanoflakes were synthesized on monolayer fluorophlogopite mica (FM˜20 μm) substrate *via* van der Waals epitaxy. The In_2Se_3 power (99.99%) used for evaporation source had been placed in the center of the horizontal tube furnace (OTL1200). A piece of FM substrate was placed downstream, about 12 cm away from the powder source, for sample growth. Under argon (Ar) gas of 50 sccm, the In_2Se_3 powder was heated to 750°C. After growth, keeping the Ar flow unchanged, we let the tubular furnace naturally cool down to ambient temperature. In addition, the PVD-In_2Se_3 nanoflakes were transferred to the facet of a fiber connector for fabricating In_2Se_3-based SA, which enhanced the laser damage threshold under high-power conditions.

The performance of the sample materials is also very important. The In_2Se_3 nanosheets were characterized, and data results are shown in **Figure 1**. **Figures 1A,B** indicate that In_2Se_3 nanoflakes have a multi-layered structure. It can be clearly observed that most of the nanoflakes have asymmetric hexagonal and irregular truncated trigonal morphology, which grow along the horizontal direction. However, due to the limitation of the heating rate of the tube furnace, the homogeneity of the deposited nanoflakes was weakened. Most of the nanoflakes show uniform thickness across the lateral dimension. From the inset of **Figure 1A**, the stoichiometric ratio of Se (51.43%) and In (34.80%) was about 3:2. The Raman result is displayed in **Figure 1C**. Apparently, three peaks at˜107,˜172, and ˜205 cm^{-1} are considered to be done by A_1 (LO + TO), A_1 (TO), and A_1 (LO) phonon modes of In_2Se_3 [42], which evidently prove that we successfully synthesized the In_2Se_3 nanoflakes [43, 44]. Diffraction peaks including (004), (006), (106), (0010), (1115), and (1118) were detected, as shown in **Figure 1D**. Compared with bulk In_2Se_3, the intensity of (006) peak is relatively higher and shows that the In_2Se_3 nanoflakes exhibit a well-layered structure. This further indicates that the In_2Se_3 nanoflakes grown with the PVD method have good uniformity and high crystallinity.

The linear absorption property is shown in **Figure 2A**. The In_2Se_3 SA has a higher transmission of 93% at 1,560 nm. As can be seen from **Figure 2A**, the linear transmission exhibits some fluctuation fringes. This phenomenon may be attributed to the interference due to the thickness of the sample. Moreover, through a power-dependent transmission technique, the nonlinear absorption properties of the In_2Se_3 SA were measured, and the experimental setup is the same as that in our previous work [46]. The final result is depicted in **Figure 2B**, where the modulation depth of 19% and the saturable intensity of 7.9 MW/ cm^2 are estimated. Due to the good uniformity of the In_2Se_3 nanoflakes, the In_2Se_3 SA exhibits a high modulation depth [47]. It has been demonstrated that SAs with a large modulation depth is beneficial to generate mode-locked ultrafast pulses with a larger single-pulse energy [48]. Therefore, In_2Se_3 prepared by the PVD method was regarded as an excellent SA to realize high-power and large-energy pulse generation.

EXPERIMENTAL SETUP

The typical experimental arrangements of the proposed PVD-In_2Se_3 EDFL are shown in **Figure 3**. Two laser diodes (LD, 976 nm) were used as a pump source, and the final highest output power was 1,838 mW. Two wavelength division multiplexer couplers were employed to couple the pump laser into the ring cavity. The highly erbium-doped fiber served as the gain medium. Meanwhile, a polarization-insensitive isolator (PI-ISO) retained the unidirectional laser operation in the ring cavity, and two polarization controllers (PCs) were connected into the laser cavity to be used to control the polarization state of the laser cavity. A 40:60 optical coupler was used to collect the output laser beam. Additionally, in order to improve the output stability of the cavity and adjust the net dispersion value in the cavity to achieve the various soliton phenomena more easily, a single-

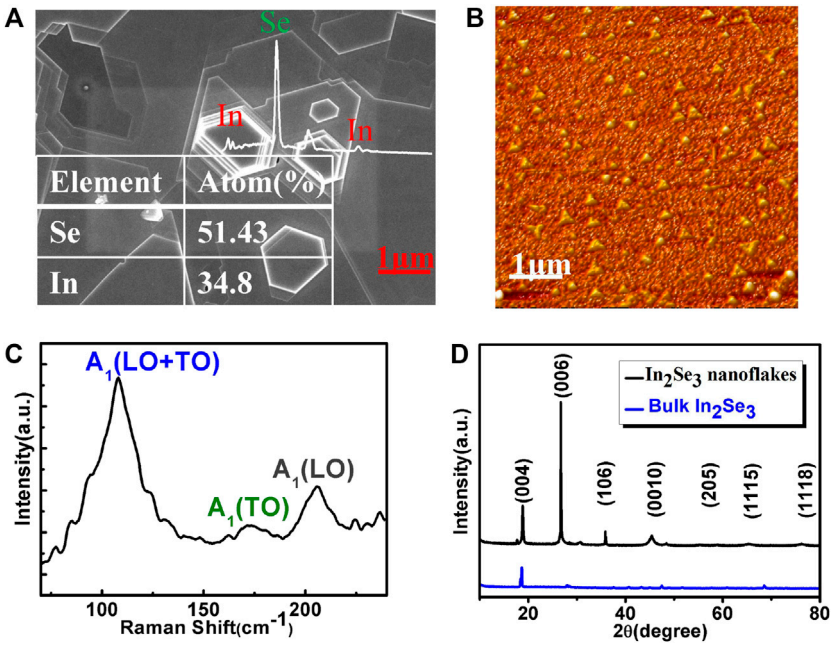

FIGURE 1 | (A) SEM image of the prepared In_2Se_3 nanoflakes (inset: energy-dispersive X-ray spectroscopy of the sample). **(B)** Atomic force microscopy image of In_2Se_3 nanoflakes. **(C)** Raman spectrum of the prepared In_2Se_3 nanoflakes. **(D)** XRD analysis of the In_2Se_3 nanoflakes.

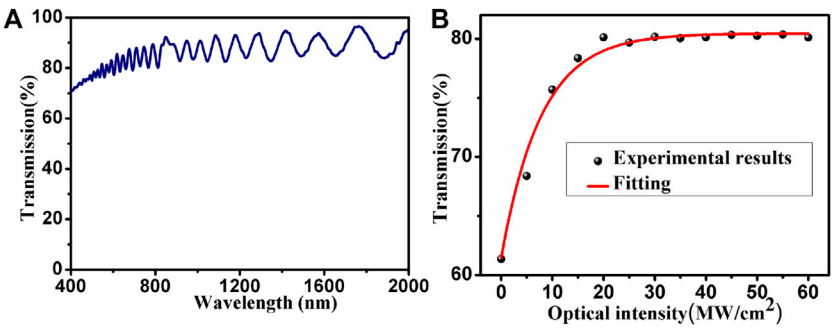

FIGURE 2 | (A) Linear transmission spectrum of In_2Se_3-FM. **(B)** The nonlinear saturable absorption curve of the In_2Se_3.

mode fiber was inserted between SA and PI-ISO in the ring laser cavity. The whole length of the proposed laser cavity is about 119 m, and the total net dispersion in the cavity is calculated as being about -2.61 ps^2.

EXPERIMENTAL RESULTS AND DISCUSSIONS

As is known to all, owing to the Kerr effect, self-mode-locked or Q-switching often occurs in the ring fiber laser cavity. Therefore, at the beginning of the experiment, we inserted a pure FM substrate without a saturated absorber into the ring laser cavity and inspected if Q-switched or self-mode-locked operations were not observed, which showed that the pure FM substrate did not produce a Kerr effect and a saturated absorption effect in the ring laser cavity. Then, we connected the In_2Se_3 SA to the EDFL system and obtained mode-locked operations. The insertion loss of the proposed cavity was calculated as 0.95 dB. Thus, the relatively large insertion loss and the high output coupling ratio caused the laser threshold to be relatively high. By maintaining the pump power at 1,838 mW for 5 or 6 h (maybe a little short), a stable mode-locked output can always be obtained, which showed that PVD-In_2Se_3 SA had a high

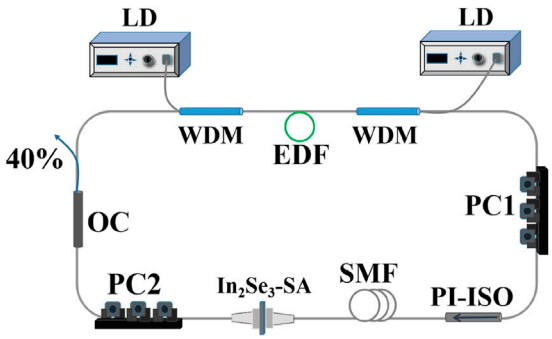

FIGURE 3 | Experimental schematic of the mode-locked erbium-doped fiber laser.

stability. What is more, no material damage was found. It can be proved that the laser damage threshold of the prepared In_2Se_3 SA was relatively high. In general, within the mode-locked laser cavity, the balance between various nonlinear optical effects, the total laser gain and loss, and the net dispersion value of the cavity contributed to the formation of different soliton generations. Bright pulses and dark–bright pulses were observed successfully by adjusting the PCs in this proposed cavity. We will discuss the two mode-locked operations in detail.

Bright Pulses

The bright pulses can be obtained easily by adjusting the PCs upon the pump power to 313 mW. Here we mainly discussed the bright pulse output characteristics, where the pump power is set as 1,838 mW, as shown in **Figure 4**. **Figure 4A** shows an oscilloscope trace of a single bright pulse with the full-width at half-maximum of 15.3 ns, which can be attributed to the large net dispersion. The inset of **Figure 4A** illustrates the pulse train with 1.718 MHz fundamental frequency, corresponding to a period of 582.8 ns, which demonstrates a stable mode-locked state. **Figure 4B** shows the optical spectrum of the dual-wavelength bright pulse with the central wavelength located at 1,559.436 and 1,560.974 nm, which is similar to the previous report [49]. However, we have not observed Kelly sidebands in the spectrum, thus proving that the EDFL operation mode was not a conventional soliton regime. The large dispersion in the experiment is one of the causes of the disappearance of the Kelly sideband [50]. Additionally, the stability issue of the passively mode-locked is an important parameter limiting the practical application of the laser. **Figure 4C** exhibits the radiofrequency (RF) spectrum of the dual-wavelength bright pulse. The peak of the fundamental frequency locates at 1.718 MHz with a signal-to-noise ratio (SNR) of 42 dB, which further indicates the relative stability of bright pulse. The average output power and single pulse energy under a different pump power are recorded in **Figure 4D**. In the case of pump power setting at 1,838 mW, the average output power was measured to be 172.4 mW and single pulse energy was 101 nJ. The high output power generation could be explained by the following aspects: (1) differently from the 2D materials prepared by other methods, such as ME and CVD, PVD-In_2Se_3 exhibits uniform thickness and high crystallinity of nanosheets and (2) PVD-In_2Se_3 SA displays excellent nonlinear optical properties—for example, larger modulation depth. In general, the lasers that operate in a negative dispersion cavity would generate conventional soliton. Limited by a soliton area theorem, the pulse energy would not

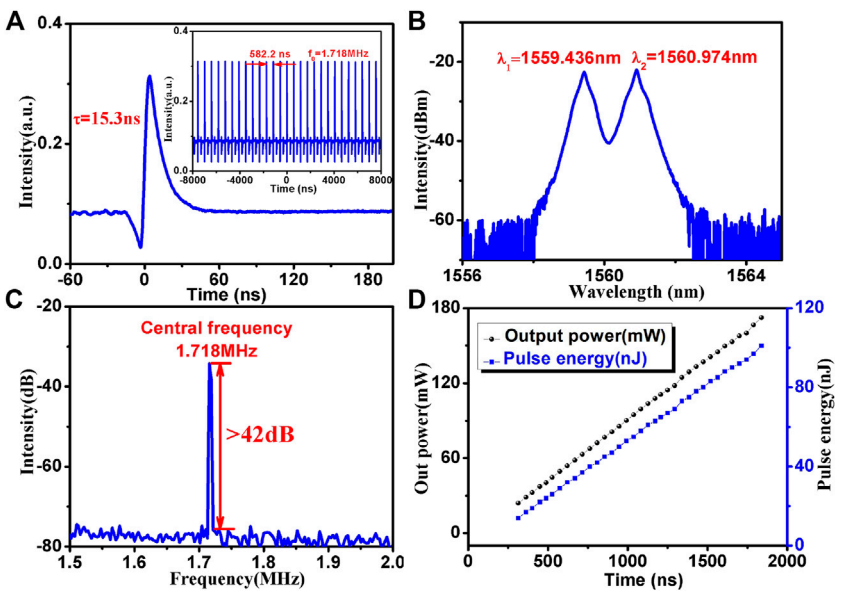

FIGURE 4 | (A) Single pulse of the bright pulse (inset: typical pulse train). **(B)** The output optical spectrum. **(C)** RF spectrum. **(D)** Pulse energy and average output power *versus* pump power.

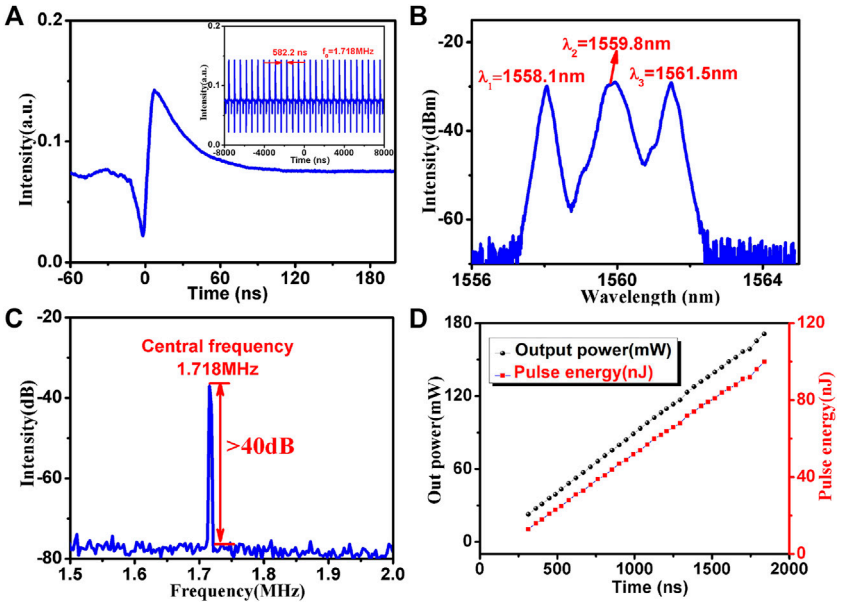

FIGURE 5 | (A) Single pulse profile of the dark-bright pulse and the inset shows the typical pulse train. **(B)** Output spectrum. **(C)** Radiofrequency spectrum. **(D)** Average output power and pulse energy.

survive above 0.1 nJ. However, according to previous reports, Yan *et al.* and Wang *et al.* achieved a soliton pulse with a single pulse energy of 2.03, 2.14, and 128.3 nJ in a negative dispersion cavity, respectively [42, 48, 50]. In our experiment, although the single pulse energy reached up to 101 nJ, but the peak power remained almost immutable due to pulse broadening caused by the large dispersion. In addition, it is well known that mode-locked lasers could operate in different soliton states under the interaction of dispersion, nonlinearity, gain, and loss. In the experiment, due to the lack of an autocorrelator, the soliton state cannot be measured. However, since the pulse obtained in our experiment was not a traditional soliton pulse, according to previous reports [51, 52], the displayed value of the oscilloscope was the real value of the pulse width. Obviously, compared with the previous work, the highest average output power was obtained and was very competitive among the reported fiber lasers based on In_2Se_3 SA in our work. The experiment results demonstrated that PVD-In_2Se_3 SA had prominent advantages in obtaining stable pulse generation with high output power.

Dark–Bright Pulse Pairs

`By further controlling the PCs, we can observe the stable dark–bright pulse pairs with 1,838 mW pump power. **Figure 5** depicts a dark–bright pulse mode locking state of the proposed fiber laser. The corresponding single dark–bright pulse pair is shown in **Figure 5A**. The depth of the dark pulse and that of the bright pulse are nearly equal in a uniform continuous wave background. The inset in **Figure 5A** shows a typical dark–bright pulse pair train with a fundamental frequency of 1.718 MHz. As can be seen from **Figure 5B**, a triple-wavelength dark–bright pulse pair can also be achieved, and spectral centers were located at 1,558.1, 1,559.8, and 1,561.5 nm, with wavelength spacing per laser wavelength of 1.7 nm, respectively. In addition, no Kelly sidebands were observed in the spectrum, similar to previous reports [53, 54]. **Figure 5C** presents the RF spectrum of the dark–bright pulse pair with a SNR of 40 dB, which indicates that a relatively stable mode-locked operation was achieved. As shown in **Figure 5D**, the maximum average output power was 171.3 mW under the pump power of 1,838 mW, corresponding to the optical conversion efficiency of 9.32%. The largest energy of the dark–bright pulse is calculated to be about 100 nJ, which is the total pulse energy of the dark–bright pulses. Other researchers had done a similar work [55, 56]. As is known, the formation of the dark–bright pulse pairs may resulted in the cross-phase modulation effect [57]. In our opinion, the formation of a dark–bright pulse pair is not only owing to the cross-phase modulation [58, 59] but also due to the interaction of the nonlinear refractivity of In_2Se_3 nanoflakes with high nonlinear effects that resulted in high-power laser cavity. Moreover, when the pump power increases, triple-wavelength mode-locked pulse generated benefits from a combination of the high nonlinearity of In_2Se_3 nanoflakes and the spectral filtering effect in laser cavity. Regrettably, owing to the lack of a tunable filter, the polarization

characteristics of the dark–bright pulse pair were not further analyzed. In addition, no pulse pairs were observed despite adjusting the PCs when the In_2Se_3-FM SA was taken away. It can be confirmed that In_2Se_3 SA is an effective saturable absorber for stable passively mode-locked operation.

CONCLUSION

In summary, due to variations in birefringence and high nonlinearity of the laser cavity, a multiwavelength output can be generated. Finally, we successfully obtained two stable soliton pulses with average output power of 172.4 and 171.3 mW and single pulse energy of 101 and 100 nJ, respectively, in a passively mode-locked EDFL using PVD-In_2Se_3 as the saturable absorber. Besides this, a triple-wavelength dark–bright pulse pair operation with highest output power and maximum pulse energy was also first observed. All in all, the type of pulse laser based on few-layer bismuthene will provide a new reference resource for obtaining a large-energy, high-power output in the mode-locked fiber lasers and its application in optical fiber communication, spectral analysis, and pump probe experiment.

DATA AVAILABILITY STATEMENT

The raw data supporting the conclusions of this article will be made available by the authors without undue reservation.

AUTHOR CONTRIBUTIONS

CZ and BM contributed to conception and design of the study. HZ and CL performed the analysis. QW wrote the first draft of the manuscript. XH wrote sections of the manuscript. All authors contributed to manuscript revision and read and approved the submitted version.

FUNDING

This study was supported by the National Natural Science Foundation of China (11974222, 11774208, and 11804200) and a Project of Shandong Province Higher Educational Science and Technology Program (J18KZ011).

REFERENCES

1. Guo S, Zhang Y, Ge Y, Zhang S, Zeng H, Zhang H. 2D V-V Binary Materials: Status and Challenges. *Adv Mater* (2019) 31:1902352. doi:10.1002/adma.201902352
2. Jiang X, Zhang L, Liu S, Zhang Y, He Z, Li W, et al. Ultrathin Metal-Organic Framework: An Emerging Broadband Nonlinear Optical Material for Ultrafast Photonics. *Adv Opt Mater* (2018) 6:1800561. doi:10.1002/adom.201800561
3. Xu Y, Shi Z, Shi X, Zhang K, Zhang H. Recent Progress in Black Phosphorus and Black-Phosphorus-Analogue Materials: Properties, Synthesis and Applications. *Nanoscale* (2019) 11:14491–527. doi:10.1039/c9nr04348a
4. Lu J, Zhang K, Liu XF, Zhang H, Sum TC, Castro Neto AH, et al. Order-disorder Transition in a Two-Dimensional boron-carbon-nitride alloy. *Nat Commun* (2013) 4:2681–7. doi:10.1038/ncomms3681
5. Xie H, Li Z, Sun Z, Shao J, Yu X-F, Guo Z, et al. Metabolizable Ultrathin Bi2Se3Nanosheets in Imaging-Guided Photothermal Therapy. *Small* (2016) 12:4136–45. doi:10.1002/smll.201601050
6. Lu L, Tang X, Cao R, Wu L, Li Z, Jing G, et al. Broadband Nonlinear Optical Response in Few-Layer Antimonene and Antimonene Quantum Dots: A Promising Optical Kerr media with Enhanced Stability. *Adv Opt Mater* (2017) 5:1700301. doi:10.1002/adom.201700301
7. Li X, Zhang S, Liu J, Yang Z. Using Reverse Saturable Absorption to Boost Broadband Noise-like Pulses. *J Lightwave Technol* (2020) 38(14): 3769–74. doi:10.1109/jlt.2020.2977272
8. Zhang H, Bao Q, Tang D, Zhao L, Loh K. Large Energy Soliton Erbium-Doped Fiber Laser with a Graphene-Polymer Composite Mode Locker. *Appl Phys Lett* (2009) 95:141103. doi:10.1063/1.3244206
9. Li G, Ma K, Jiao Y, Jiang Q, Zhang X, Zhang Z, et al. Performance Enhancement of DFBL Based Near-infrared CH 4 Telemetry System Using a Focus Tunable Lens. *Microw Opt Technol Lett* (2021) 63: 1147–51. doi:10.1002/mop.32733
10. Yu J, Li C, Qiu X, Chen H, Zhang W. Defect Measurement Using the Laser Ultrasonic Technique Based on Power Spectral Density Analysis and Wavelet Packet Energy. *Microw Opt Technol Lett* (2021) 63:2079–84. doi:10.1002/mop.32888
11. Feng W, Qu Y, Gao Y, Ma Y. Advances in Fiber-based Quartz Enhanced Photoacoustic Spectroscopy for Trace Gas Sensing. *Microw Opt Technol Lett* (2021) 63:2031–9. doi:10.1002/mop.32841
12. Lang Z, Qiao S, He Y, Ma Y. Quartz Tuning fork-based Demodulation of an Acoustic Signal Induced by Photo-Thermo-Elastic Energy Conversion. *Photoacoustics.* (2021) 22:100272. doi:10.1016/j.pacs.2021.100272
13. Ma Y, Hu Y, Qiao S, He Y, Tittel FK. Trace Gas Sensing Based on Multi-Quartz-Enhanced Photothermal Spectroscopy. *Photoacoustics.* (2020) 20: 100206. doi:10.1016/j.pacs.2020.100206
14. Qiao S, Ma Y, He Y, Patimisco P, Sampaolo A, Spagnolo V. Ppt Level Carbon Monoxide Detection Based on Light-Induced Thermoelastic Spectroscopy Exploring Custom Quartz Tuning forks and a Mid-infrared QCL. *Opt Express* (2021) 29:25100–8. doi:10.1364/OE.434128
15. Jiang T, Yin K, Wang C, You J, Ouyang H, Miao R, et al. Ultrafast Fiber Lasers Mode-Locked by Two-Dimensional Materials: Review and prospect. *Photon Res* (2020) 8(1):78–90. doi:10.1364/prj.8.000078
16. Guo B, Xiao QL, Wang SH, Zhang H. 2D Layered Materials: Synthesis, Nonlinear Optical Properties, and Device Applications. *Laser Photon Rev* (2019) 13(12):1800327. doi:10.1002/lpor.201800327
17. Pawliszewska M, Martynkien T, Przewłoka A, Sotor J. Dispersion-managed Ho-Doped Fiber Laser Mode-Locked with a Graphene Saturable Absorber. *Opt Lett* (2018) 43(1):38–41. doi:10.1364/ol.43.000038
18. Lau KY, Abu Bakar MH, Muhammad FD, Latif AA, Omar MF, Yusoff Z, et al. Dual-wavelength, Mode-Locked Erbium-Doped Fiber Laser Employing a Graphene/polymethyl-Methacrylate Saturable Absorber. *Opt Express* (2018) 26(10):12790–800. doi:10.1364/oe.26.012790
19. Khazaeizhad R, Kassani SH, Jeong H, Yeom D-I, Oh K. Mode-locking of Er-Doped Fiber Laser Using a Multilayer MoS_2 Thin Film as a Saturable Absorber in Both Anomalous and normal Dispersion Regimes. *Opt Express* (2014) 22(19):23732–42. doi:10.1364/oe.22.023732
20. Yang HR, Liu XM. WS_2-Clad Microfiber Saturable Absorber for High-Energy Rectangular Pulse Fiber Laser. *IEEE J Sel Top Quan Electron.* (2018) 24(3): 0900807. doi:10.1109/jstqe.2017.2757142
21. Du J, Wang Q, Jiang G, Xu C, Zhao C, Xiang Y, et al. Ytterbium-doped Fiber Laser Passively Mode Locked by Few-Layer Molybdenum Disulfide (MoS2) Saturable Absorber Functioned with Evanescent Field Interaction. *Sci Rep* (2014) 4:6346. doi:10.1038/srep06346
22. Mao D, She X, Du B, Yang D, Zhang W, Song K, et al. Erbium-doped Fiber Laser Passively Mode Locked with Few-Layer WSe2/MoSe2 Nanosheets. *Sci Rep* (2016) 6:23583. doi:10.1038/srep23583
23. Luo Z, Li Y, Zhong M, Huang Y, Wan X, Peng J, et al. Nonlinear Optical Absorption of Few-Layer Molybdenum Diselenide (MoSe2) for Passively Mode-Locked Soliton Fiber Laser. *Photon Res.* (2015) 3:79–86. doi:10.1364/prj.3.000a79

24. Liu H, Zheng X-W, Liu M, Zhao N, Luo A-P, Luo Z-C, et al. Femtosecond Pulse Generation from a Topological Insulator Mode-Locked Fiber Laser. *Opt Express* (2014) 22(6):6868–73. doi:10.1364/oe.22.006868
25. Lee J, Koo J, Jhon YM, Lee JH. A Femtosecond Pulse Erbium Fiber Laser Incorporating a Saturable Absorber Based on Bulk-Structured Bi_2Te_3 Topological Insulator. *Opt Express* (2014) 22(5):6165–73. doi:10.1364/oe.22.006165
26. Sotor J, Sobon G, Macherzynski W, Abramski KM. Harmonically Mode-Locked Er-Doped Fiber Laser Based on a Sb2Te3topological Insulator Saturable Absorber. *Laser Phys Lett* (2014) 11(5):055102. doi:10.1088/1612-2011/11/5/055102
27. Guo B, Wang S-H, Wu Z-X, Wang Z-X, Wang D-H, Huang H, et al. Sub-200 Fs Soliton Mode-Locked Fiber Laser Based on Bismuthene Saturable Absorber. *Opt Express* (2018) 26(18):22750–60. doi:10.1364/oe.26.022750
28. Song Y, Liang Z, Jiang X, Chen Y, Li Z, Lu L, et al. Few-layer Antimonene Decorated Microfiber: Ultra-short Pulse Generation and All-Optical Thresholding with Enhanced Long Term Stability. *2d Mater* (2017) 4: 045010. doi:10.1088/2053-1583/aa87c1
29. Li P, Chen Y, Yang T, Wang Z, Lin H, Xu Y, et al. Two-Dimensional CH3NH3PbI3 Perovskite Nanosheets for Ultrafast Pulsed Fiber Lasers. *ACS Appl Mater Inter* (2017) 9:12759–65. doi:10.1021/acsami.7b01709
30. Sotor J, Sobon G, Kowalczyk M, Macherzynski W, Paletko P, Abramski KM. Ultrafast Thulium-Doped Fiber Laser Mode Locked with Black Phosphorus. *Opt Lett* (2015) 40(16):3885–8. doi:10.1364/ol.40.003885
31. Luo Z-C, Liu M, Guo Z-N, Jiang X-F, Luo A-P, Zhao C-J, et al. Microfiber-based Few-Layer Black Phosphorus Saturable Absorber for Ultra-fast Fiber Laser. *Opt Express* (2015) 23(15):20030–9. doi:10.1364/oe.23.020030
32. Al-Masoodi AHH, Yasin M, Ahmed MHM, Latiff AA, Arof H, Harun SW. Mode-locked Ytterbium-Doped Fiber Laser Using Mechanically Exfoliated Black Phosphorus as Saturable Absorber. *Optik* (2017) 147:52–8. doi:10.1016/j.ijleo.2017.08.038
33. Bao Q, Zhang H, Wang Y, Ni Z, Yan Y, Shen ZX, et al. Atomic-Layer Graphene as a Saturable Absorber for Ultrafast Pulsed Lasers. *Adv Funct Mater* (2009) 19(19):3077–83. doi:10.1002/adfm.200901007
34. Zheng Z, Zhao C, Lu S, Chen Y, Li Y, Zhang H, et al. Microwave and Optical Saturable Absorption in Graphene. *Opt Express* (2012) 20(21):23201–14. doi:10.1364/oe.20.023201
35. Alani IAM, Lokman MQ, Ahmed MHM, Al-Masoodi AHH, Latiff AA, Harun SW. A Few-Picosecond and High-Peak-Power Passively Mode-Locked Erbium-Doped Fibre Laser Based on Zinc Oxide Polyvinyl Alcohol Film Saturable Absorber. *Laser Phys* (2018) 28:075105. doi:10.1088/1555-6611/aabd24
36. Mafi E, Soudi A, Gu Y. Electronically Driven Amorphization in Phase-Change In2Se3 Nanowires. *J Phys Chem C* (2012) 116:22539–44. doi:10.1021/jp305696w
37. Li QL, Li Y, Gao J, Wang SD, Sun XH. High Performance Single In2Se3 Nanowire Photodetector. *Appl Phys Lett* (2011) 99:243105. doi:10.1063/1.3669513
38. Jacobs-Gedrim RB, Shanmugam M, Jain N, Durcan CA, Murphy MT, Murray TM, et al. Extraordinary Photoresponse in Two-Dimensional In2Se3 Nanosheets. *ACS Nano* (2014) 8(1):514–21. doi:10.1021/nn405037s
39. Popović S, Tonejc A, Gržeta-Plenković B, Čelustka B, Trojko R. Revised and New crystal Data for Indium Selenides. *J Appl Crystallogr* (1979) 12:416–20. doi:10.1107/s0021889879012863
40. Quereda J, Biele R, Rubio-Bollinger G, Agraït N, D'Agosta R, Castellanos-Gomez A. Strong Quantum Confinement Effect in the Optical Properties of Ultrathin α-In2Se3. *Adv Opt Mater* (2016) 4(12):1939–43. doi:10.1002/adom.201600365
41. Zhou J, Zeng Q, Lv D, Sun L, Niu L, Fu W, et al. Controlled Synthesis of High-Quality Monolayered α-In2Se3 via Physical Vapor Deposition. *Nano Lett* (2015) 15(10):6400–5. doi:10.1021/acs.nanolett.5b01590
42. Yan P, Jiang Z, Chen H, Yin J, Lai J, Wang J, et al. α-In2Se3 Wideband Optical Modulator for Pulsed Fiber Lasers. *Opt Lett* (2018) 43(18):4417–20. doi:10.1364/ol.43.004417
43. Feng W, Zheng W, Gao F, Chen X, Liu G, Hasan T, et al. Sensitive Electronic-Skin Strain Sensor Array Based on the Patterned Two-Dimensional α-In2Se3. *Chem Mater* (2016) 28(12):4278–83. doi:10.1021/acs.chemmater.6b01073
44. Zhou Y, Wu D, Zhu Y, Cho Y, He Q, Yang X, et al. Out-of-Plane Piezoelectricity and Ferroelectricity in Layered α-In2Se3 Nanoflakes. *Nano Lett* (2017) 17(9):5508–13. doi:10.1021/acs.nanolett.7b02198
45. Han XL, Zhang HN, Jiang SZ, Zhang C, Li DW, Guo QX, et al. Improved Laser Damage Threshold of In_2Se_3 Saturable Absorber by PVD for High-Power Mode-Locked Er-Doped Fiber Laser. *Nanomaterials* (2020) 9:1216.
46. Ming N, Tao S, Yang W, Chen Q, Sun R, Wang C, et al. Mode-locked Er-Doped Fiber Laser Based on PbS/CdS Core/shell Quantum Dots as Saturable Absorber. *Opt Express* (2018) 26(7):9017–26. doi:10.1364/oe.26.009017
47. Fu X, Qian J, Qiao X, Tan P, Peng Z. Nonlinear Saturable Absorption of Vertically Stood WS_2 Nanoplates. *Opt Lett* (2014) 39(22):6450–3. doi:10.1364/ol.39.006450
48. Wang J, Jiang Z, Chen H, Li J, Yin J, Wang J, et al. High Energy Soliton Pulse Generation by a Magnetron-Sputtering-Deposition-Grown MoTe2 Saturable Absorber. *Photon Res* (2018) 6(6):535–41. doi:10.1364/prj.6.000535
49. Guo B, Yao Y, Xiao J-J, Wang R-L, Zhang J-Y. Topological Insulator-Assisted Dual-Wavelength Fiber Laser Delivering Versatile Pulse Patterns. *IEEE J Select Top Quan Electron.* (2016) 22(2):8–15. doi:10.1109/jstqe.2015.2426951
50. Yan P, Chen H, Yin J, Xu Z, Li J, Jiang Z, et al. Large-area Tungsten Disulfide for Ultrafast Photonics. *Nanoscale* (2017) 9(5):1871–7. doi:10.1039/c6nr09183k
51. Fu S, Shang X, Zhang F, Xing F, Man Z, Zhang W, et al. Ferromagnetic Insulator Cr2Ge2Te6 as a Modulator for Generating Near-Infrared Bright-Dark Soliton Pairs. *Appl Opt* (2019) 58(33):9217–23. doi:10.1364/ao.58.009217
52. Zhao R, Wang M, Zheng Y, Xu N, Liu D, Li D. Generation of Dark-Bright-Bright Solitons in Er-Doped Fiber Laser Based on Ferromagnetic Insulator Cr2Ge2Te6. *Infrared Phys Tech* (2020) 109:103417. doi:10.1016/j.infrared.2020.103417
53. Gao J, Hu FM, Huo XD, Gao P. Bright-dark Pair in Passively Mode-Locked Fiber Laser Based on Graphene. *Laser Phys* (2014) 24(8):085104. doi:10.1088/1054-660x/24/8/085104
54. Guo B, Yao Y, Tian J-J, Zhao Y-F, Liu S, Li M, et al. Observation of Bright-Dark Soliton Pair in a Fiber Laser with Topological Insulator. *IEEE Photon Technol Lett* (2015) 27(7):701–4. doi:10.1109/lpt.2015.2390212
55. Zhao L, Xu NN, Zhao R, Shang XX, Liu XY, Zhang ZD, et al. Generation of Single-,dual-Wavelength Mode-Locked Operations Based on $ZrSe_2$ as Saturable Absorber in an Er-Doped Fiber Laser. *INFRARED PHYS TECHN* (2021) 116:103775. doi:10.1016/j.infrared.2021.103775
56. Ma P, Li J, Zhang H, Yang Z. Preparation of High-Damage Threshold WS2 Modulator and its Application for Generating High-Power Large-Energy Bright-Dark Solitons. *Infrared Phys Tech* (2020) 105:103257. doi:10.1016/j.infrared.2020.103257
57. Zhao R, Li G, Zhang B, He J. Multi-wavelength Bright-Dark Pulse Fiber Laser Based on Rhenium Disulfide. *Opt Express* (2018) 26(5):5819–26. doi:10.1364/oe.26.005819
58. Ning Q-Y, Wang S-K, Luo A-P, Lin Z-B, Luo Z-C, Xu W-C. Bright-Dark Pulse Pair in a Figure-Eight Dispersion-Managed Passively Mode-Locked Fiber Laser. *IEEE Photon J.* (2012) 4(5):1647–52. doi:10.1109/jphot.2012.2212878
59. Lisak M, Höök A, Anderson D. Symbiotic Solitary-Wave Pairs Sustained by Cross-phase Modulation in Optical Fibers. *J Opt Soc Am B* (1990) 7(5):810–4. doi:10.1364/josab.7.000810

Conflict of Interest: The authors declare that the research was conducted in the absence of any commercial or financial relationships that could be construed as a potential conflict of interest.

Publisher's Note: All claims expressed in this article are solely those of the authors and do not necessarily represent those of their affiliated organizations or those of the publisher, the editors, and the reviewers. Any product that may be evaluated in this article or claim that may be made by its manufacturer is not guaranteed or endorsed by the publisher.